International Journal of Electrical and Computer Engineering (IJECE)
Vol. 15, No. 5, October 2025, pp. 4430~4444
ISSN: 2088-8708, DOI: 10.11591/ijece.v15i5.pp4430-4444

Enhancing source currents and ensuring load voltage stability in railway electrification system via unified power quality conditions implementation

Kittaya Somsai, Jeerapong Srivichai, Veera Thanyaphirak
Department of Electrical Engineering, Faculty of Industry and Technology, Rajamangala University of Technology Isan, Sakon Nakhon Campus, Sakon Nakhon, Thailand

Article Info

Article history:

Received Dec 20, 2024
Revised Jun 4, 2025
Accepted Jun 30, 2025

Keywords:

Current balancing
Electric railway system
Harmonic current compensation
Unified power quality conditioner
Voltage enhancing

ABSTRACT

In recent years, interest in electric railway system as a transportation solution for large urban areas has grown significantly. This increased attention stems from several key advantages, including environmental friendliness, high performance, reduced maintenance costs, and lower energy expenses. Railway electrification system rely on supplying power to trains through single-phase transformers. However, these transformers can cause issues such as current imbalances and harmonics at the system connection point, which may impact critical loads. Additionally, fluctuations in source voltage can influence the system's performance. This study examines the causes of unbalanced loading in railway electrification system and introduces an innovative unified power quality conditioner (UPQC) specifically designed for integration into low-voltage railway electrification system. The proposed UPQC aims to restore current balance, minimize harmonics, and enhance overall power quality. Furthermore, it addresses the mitigation of voltage sags in the power distribution network. The simulation results generated through MATLAB programming demonstrate the UPQC's effectiveness in enhancing system performance. The findings reveal that the UPQC reduces source current imbalance to less than 1.6% and total harmonic distortion (THD) to below 4.89% across all test scenarios. Additionally, the UPQC successfully maintains a load bus voltage of 25 kV during single-phase-to-ground and unbalanced three-phase-to-ground fault conditions.

Corresponding Author:

Kittaya Somsai
Department of Electrical Engineering, Faculty of Industry and Technology, Rajamangala University of Technology Isan
Sakon Nakhon Campus, 199 Village No.3 Phang Khon-Waritchaphum Road, Phang Khon subdistrict, Phang Khon district, Sakon Nakhon, 47160, Thailand
Email: kittaya.so@rmuti.ac.th

1. INTRODUCTION

Railway electrification systems are critical to public transportation due to their ability to handle increasing passenger demand and transport goods over a wide range of distances. However, ensuring their reliability and stability as efficient transportation solutions remains a challenge, particularly regarding power quality in the power supply. These challenges are especially pronounced in long-distance, high-speed trains powered by 25–27.5 kV, 50 Hz AC systems [1]–[5]. In conventional AC traction systems, the conversion of a 115 kV three-phase grid to a 25 kV single-phase system is typically achieved using single-phase transformers [6], [7]. The V/V transformer is commonly used for this purpose due to its simple design, ease

of installation, maintenance, and straightforward control. Although V/V transformers offer certain advantages, they encounter major challenges, including negative sequence currents (NSC), harmonics, and a low power factor, all of which negatively impact the efficiency and power system' stability [8], [9].

These power quality issues are more noticeable when AC railway systems are connected to weak power grids, leading to higher operational costs and disruption to sensitive equipment, such as medical devices and database systems [10]. Problems such as voltage waveform distortion and harmonics reduce power supply efficiency and negatively affect the connected three-phase grid, especially during periods of high demand and frequent usage [11]. The single-phase, non-linear characteristics of AC railway traction loads further contributes to power quality issues, including NSC [9], [12] low power factor [13], harmonics [14], [15], and reactive power consumption [16], [17]. These problems result in energy losses in feeders, reduced transformer capacity, malfunctioning of protective relays, and errors in transmission control systems.

To enhance the power quality (PQ) parameters of railway electrification system, researchers have explored various methods over the years. Addressing NSC has been a focal point, with solutions such as specially designed transformers, including Scott, Woodbridge, impedance-matching balance, and LeBlanc transformers [18]–[23]. Reactive power compensation has been another area of focus, with static VAR compensators (SVC) [24]–[26] and static synchronous compensators (STATCOM) [27], [28] widely utilized. While SVCs dynamically compensate reactive power, they generate harmonics, which STATCOMs can mitigate. Single-phase STATCOMs are well-suited for railway feeders with low isolation needs, while three-phase STATCOMs can dynamically address NSC but require large step-down transformers.

Additional methods, such as railway power conditioners (RPC) [29]–[32] and active power quality compensators (APQC) [33], have demonstrated potential in addressing power quality issues. While RPCs effectively compensate for NSC, harmonics, and low power factors, they are limited by their complexity and lack of flexibility. The hybrid railway power compensator (HRPC) [34]–[36], which integrates RPCs with passive filters or SVCs, offers some improvement in power quality. However, HRPCs still face challenges, such as control complexity, overcompensation, and resonance, which degrade system performance [37]. Notably, most of these solutions fail to mitigate voltage sags resulting from single-phase or three-phase faults in railway systems.

The unified power quality conditioner (UPQC) is a promising alternative for resolving power quality problems in the AC electrification system of railway traction. By employing series and parallel converters, UPQC can address voltage and current disturbances while mitigating harmonic distortions. Recent studies have focused on designing V/V-connected UPQC to eliminate harmonics and NSC in railway systems [38]. Other research has emphasized integrating renewable energy sources and energy storage systems into UPQC designs to enhance power quality and utilize energy recovered during braking operations [39]. Modern research trends also highlight the potential of UPQC for improving railway power quality through intelligent control systems. Artificial intelligence (AI) based control techniques have shown promise in enhancing system performance, reducing harmonics, and improving overall power quality [40], [41]. However, the high cost of UPQC, especially for high-voltage three-phase systems, poses a significant barrier to widespread implementation.

This study introduces a novel UPQC application tailored for railway systems, specifically designed for connection to the low-voltage side near the load to enhance control and compensation efficiency. The proposed UPQC effectively reduces current imbalance and harmonics while maintaining voltage stability during single-phase and three-phase faults in the power grid. An in-depth analysis and control system design for the UPQC demonstrate its ability to efficiently mitigate power quality issues with high precision. The results of MATLAB simulation validate the performance of the proposed UPQC in improving power quality and operational stability in railway systems.

2. PROPOSED SYSTEM

2.1. Electric railway system with UPQC

Figure 1 shows schematic diagram of the proposed compensator designed to balance currents and regulate voltage within the railway electrification system. It depicts the connection of traction substations to the power grid at the point of common coupling (PCC) through a V/V transformer. The compensator employed in this study is the UPQC, which is installed between the traction side and the low-voltage side of the V/V transformer to achieve current balancing and voltage regulation. Figure 2 provides a detailed view of the UPQC configuration tailored specifically for these purposes in the railway system.

In conventional practice, the V/V transformer in traction substations steps down the three-phase 115 kV from the source system to two single-phase traction feeders operating at 25 kV. The UPQC comprises two converters that share a DC-link capacitor, which helps maintain a stable DC-link voltage. One converter, called the series converter, is linked to the traction feeder through a three-phase transformer, while

the other, the shunt converter, is connected in parallel to the feeder via a separate three-phase step-down transformer.

As illustrated in Figure 2, the shunt converter is strategically placed close to the load, which serves as the power supply station for trains, while the series converter is positioned near the V/V transformer. This configuration is intentional, as the shunt converter is well-suited for mitigating current imbalances caused by variable loads, while the series converter is designed to shield the loads from voltage fluctuations originating from the power source. By employing an effective control strategy, the UPQC can dynamically adjust the output currents and voltages of both converters. This dual capability allows the series converter to address voltage sags at the load while the shunt converter compensates for current imbalances, thereby significantly enhancing the overall system efficiency and stability.

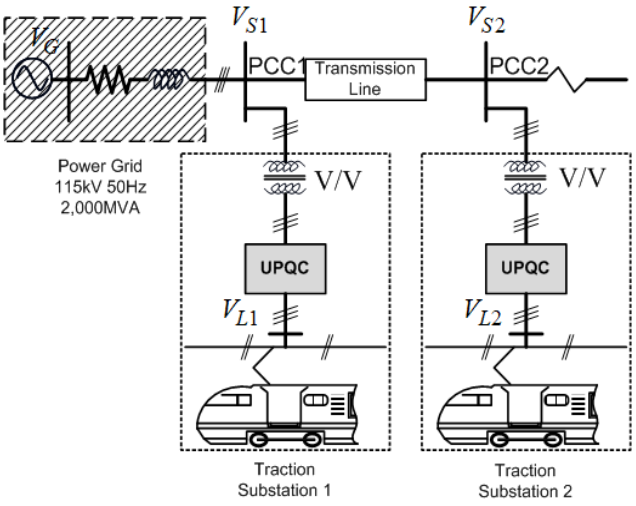

Figure 1. Schematic diagram of the electric railway system with UPQC

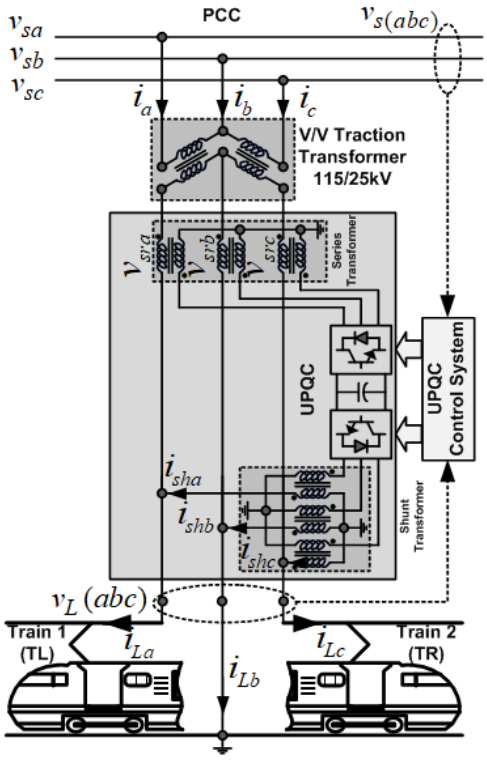

Figure 2. Configuration of the electric railway system with UPQC

2.2. Principle of operation of the UPQC

The test setup for the electric railway system configuration integrated with the UPQC is shown in Figure 2. Further details are presented in the single-line diagram presented in Figure 3. This diagram represents the system components, including the power system, the V/V transformer, a railway load consisting of two trains, the right-shunt UPQC device, and the UPQC control system.

The main components of the UPQC in the described configuration are the series and shunt converters, which share a DC-link capacitor. The operational mechanism of the UPQC for achieving current balancing and voltage enhancement in the railway electrification system is outlined as follows. The series converter operates as a voltage source converter (VSC) and is connected in series with the traction feeder. Its role is to inject an unbalanced series voltage into the traction feeder to compensate for unbalanced load voltages and to regulate the load voltage to the required level. Similarly, the shunt converter, also a VSC, is connected in parallel with the traction feeder. Its function is to inject unbalanced currents into the traction feeder, thereby compensating for unbalanced source currents at the PCC, while also maintaining the DC-link voltage at the desired level.

The effectiveness of the UPQC depends heavily on the control strategies implemented for its operation. The roles of both the series and shunt converters have been clearly defined, providing the basis for their respective control strategies. The UPQC employs two distinct control strategies: one for the series converter and another for the shunt converter. By effectively coordinating these strategies, the UPQC ensures proper compensation of unbalanced source currents and maintains regulated voltages within the railway electrification system.

As shown in Figure 3, the current originating from the source and passing through the source resistance R_s and inductance L_s is denoted as i_s. The voltage provided to the traction station, denoted as v_{sL}, is reduced via a V/V transformer with a transformation ratio of a_v. For the series converter, the current passing through the series transformer to the load is denoted as i_{sr}, while the current entering the series converter is represented by i_{srC}. The voltage from the series converter that is supplied to the load is v_{srL}. This voltage, v_{srL}, is related to the output voltage of the series converter, v_{srC}, by the series transformer ratio a_{sr}. It can be regulated by modifying the control signal u_{sr}.

For the shunt converter, the voltage at the PCC is represented as v_{sh}, while the current of the shunt converter that passes through its resistance R_{sh} and inductance L_{sh}, is denoted as i_{sh}. The current entering the shunt converter is also represented as i_{sh}. This current, i_{sh}, is utilized to compensate for unbalanced source currents and to reduce harmonics in the supply current. The relationship between i_{sh} and i_{shC} is defined by the shunt transformer ratio a_{sh}. The adjustment of i_{sh} is achieved by controlling the voltage across the shunt converter, v_{shC}, through the control signal u_{sh}. Nonetheless, to control the voltage across both the series and shunt converters (v_{srC} and v_{shC}), it is essential to depend on the DC voltage, v_{dc}, on the DC side. However, controlling the voltage across both the series and shunt converters (v_{srC} and v_{shC}) relies on the DC voltage v_{dc} on the DC side.

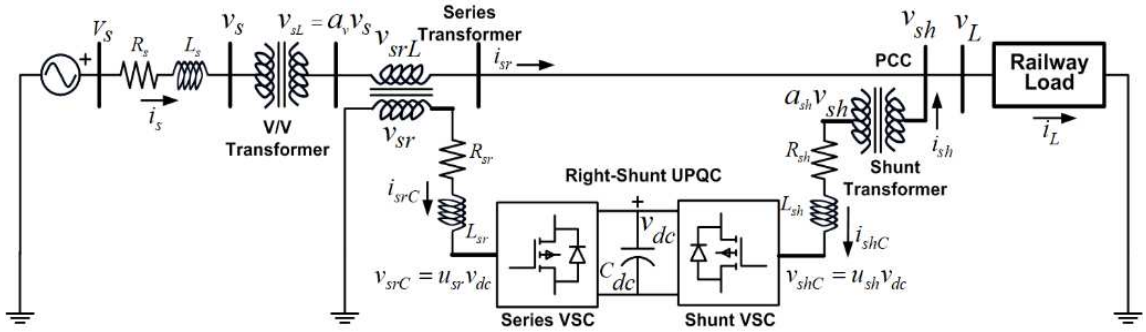

Figure 3. Single-line diagram of the system

3. CONTROL STRATEGIES OF UPQC

The UPQC control system employs various theoretical approaches, including instantaneous power theory [42], instantaneous symmetrical components theory [43], and synchronous rotating reference frame theory [44]. This study, however, focuses specifically on reducing unbalanced source currents using instantaneous power theory and achieving voltage regulation through the synchronous rotating reference frame theory.

3.1. Control of shunt converter

The shunt converter is in charge of correcting unbalanced source currents and maintaining the DC-link voltage at the desired level. Additionally, it can filter out harmonic currents. The instantaneous power theory or the p-q theory, which has been previously applied in D-STATCOM devices for harmonic filtering and improving power quality, is now utilized to control the shunt converter in this UPQC. One of the primary uses of the p-q theory is to address unwanted currents, such as harmonic and unbalanced currents.

$$\begin{bmatrix} v_{L0} \\ v_{L\alpha} \\ v_{L\beta} \end{bmatrix} = \sqrt{\frac{2}{3}} \begin{bmatrix} \frac{1}{2} & \frac{1}{2} & \frac{1}{2} \\ 1 & -\frac{1}{2} & -\frac{1}{2} \\ 0 & \frac{\sqrt{3}}{2} & -\frac{\sqrt{3}}{2} \end{bmatrix} \begin{bmatrix} v_{La} \\ v_{Lb} \\ v_{Lc} \end{bmatrix} \tag{1}$$

$$\begin{bmatrix} i_{L0} \\ i_{L\alpha} \\ i_{L\beta} \end{bmatrix} = \sqrt{\frac{2}{3}} \begin{bmatrix} \frac{1}{2} & \frac{1}{2} & \frac{1}{2} \\ 1 & -\frac{1}{2} & -\frac{1}{2} \\ 0 & \frac{\sqrt{3}}{2} & -\frac{\sqrt{3}}{2} \end{bmatrix} \begin{bmatrix} i_{La} \\ i_{Lb} \\ i_{Lc} \end{bmatrix} \tag{2}$$

$$\begin{bmatrix} p_L \\ q_L \end{bmatrix} = \begin{bmatrix} i_{L\alpha} & i_{L\beta} \\ -i_{L\beta} & i_{L\alpha} \end{bmatrix} \begin{bmatrix} v_{L\alpha} \\ v_{L\beta} \end{bmatrix} \tag{3}$$

Figure 4 illustrates the control strategy designed for shunt converter. This approach utilizes the p-q theory, which incorporates the $\alpha\beta0$ transformation or Clarke transformation [42]. This transformation uses a real matrix to convert three-phase voltages and currents into $\alpha\beta0$ axes, as defined in equations (1) and (2). The load real power (p_L) is divided into its mean component ($\bar{p}_L$) and oscillating component ($\tilde{p}_L$). Similarly, the reactive power of the load (q_L) is divided into its mean ($\bar{q}_L$) and oscillating ($\tilde{q}_L$) components. For simplicity, this study focuses on a three-phase, three-wire system, where zero-sequence voltage and current components are absent. Under this condition, the p_L and q_L of the load can be derived from (3).

In this research, the shunt converter of the UPQC corrects for the components $\tilde{p}_L$ and $\tilde{q}_L$, ensuring that only the $\bar{p}_L$ is taken from the power system. As a result, the constant instantaneous power control strategy provides optimal compensation for power flow, even in the presence of non-sinusoidal or unbalanced system currents. The real power of the electric railway system, represented as a nonlinear load in Figure 2, must be continuously monitored and divided into $\bar{p}_L$ and $\tilde{p}_L$ components using a mean function.

Additionally, the inclusion of a DC voltage regulator into the shunt converter control strategy, as shown in Figure 4, is essential. A small quantity of power ($\bar{p}_{loss}$) must be drawn continuously from the power system to compensate for the losses in the PWM converter. If not, the DC capacitor would supply this energy, leading to its gradual discharge. This highlights the need to maintain the DC voltage at a constant level higher than the peak AC-bus voltage, which is achieved using a PI controller to control the DC voltage.

Thus, the shunt converter must supply the oscillating components of the instantaneous active and reactive currents of the load. These currents can be determined using (4) for their reference values in the $\alpha\beta$ axis. The reference currents are then transformed back into the abc reference frame, as described in (5), for further use in the control system.

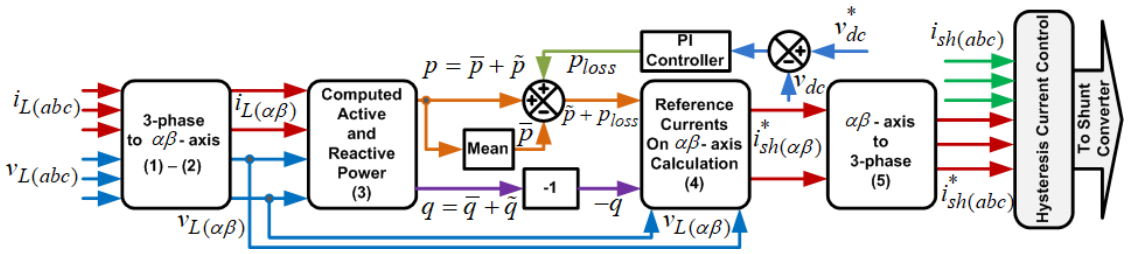

Figure 4. Control block diagram of shunt converter of UPQC

$$\begin{bmatrix} i^*_{sh\alpha} \\ i^*_{sh\beta} \end{bmatrix} = \frac{1}{v^2_{L\alpha}+v^2_{L\beta}} \begin{bmatrix} v_{L\alpha} & v_{L\beta} \\ v_{L\beta} & -v_{L\alpha} \end{bmatrix} \begin{bmatrix} -\tilde{p} + \overline{p_{loss}} \\ -q \end{bmatrix} \tag{4}$$

$$\begin{bmatrix} i^*_{sha} \\ i^*_{shb} \\ i^*_{shc} \end{bmatrix} = \sqrt{\frac{2}{3}} \begin{bmatrix} 1 & 0 \\ -\frac{1}{2} & \frac{\sqrt{3}}{2} \\ -\frac{1}{2} & -\frac{\sqrt{3}}{2} \end{bmatrix} \begin{bmatrix} i^*_{sh\alpha} \\ i^*_{sh\beta} \end{bmatrix} \quad (5)$$

The gate pulses which required for shunt converter are produced by hysteresis current control. Comparing between the fundamental current ($i_{sh(abc)}$) and reference signal current with the hysteresis band ($i^*_{sh(abc)} \pm h$) is used to generate the gate pulses. The gate pulses required for the shunt converter are generated using hysteresis current control. This method compares the actual fundamental current $i_{sh(abc)}$ with the reference current signal within a specified hysteresis band ($i^*_{sh(abc)} \pm h$) to produce the gate pulses.

3.2. Control of series converter

The series converter is in charge of compensating the load voltage and regulating it to the desired level. To manage voltage imbalances and maintain stable operational voltage, this study applies the synchronous rotating reference frame (SRF) theory. The SRF theory involves transforming three-phase signals (*abc*) into the *dq0* rotating reference frame using the Park transformation. This transformation relies on the initial alignment of the *dq0* frame at time *t*=0, corresponding to the position of the rotating reference frame determined by the angular velocity (ω). This approach facilitates the conversion of AC waveforms into DC signals. However, in this study, the zero-sequence component is neglected, as the focus is on a three-phase three-wire system.

The unbalanced voltage in the electric railway system is primarily due to the NSC within the synchronous rotating reference frame, posing a significant challenge for voltage compensation. To mitigate this issue, the series converter of the UPQC is employed to compensate for the NSC in the *dq* domain, while the PSC in the *dq* domain is employed to control the load voltage to the desired level.

Figure 5 presents the diagram of the series converter control. In this diagram, the three-phase load voltages (v_{La}, v_{Lb} and v_{Lc}) are transformed into *dq*-PSC ($v_{Ld(+)}$ and $v_{Lq(+)}$) and *dq*-NSC ($v_{Ld(-)}$ and $v_{Lq(-)}$) using (6) and (7), respectively. The orientation of the rotating reference frame (ωt) in these equations is determined by a phase-locked loop (PLL), which calculates the angular velocity of the voltage $v_{s(abc)}$.

$$\begin{bmatrix} v_{Ld(+)} \\ v_{Lq(+)} \\ v_{L0(+)} \end{bmatrix} = \frac{2}{3} \begin{bmatrix} \cos(\omega t) & \cos(\omega t - \frac{2\pi}{3}) & \cos(\omega t + \frac{2\pi}{3}) \\ \sin(\omega t) & -\sin(\omega t - \frac{2\pi}{3}) & -\sin(\omega t + \frac{2\pi}{3}) \\ \frac{1}{2} & \frac{1}{2} & \frac{1}{2} \end{bmatrix} \begin{bmatrix} v_{La} \\ v_{Lb} \\ v_{Lc} \end{bmatrix} \quad (6)$$

$$\begin{bmatrix} v_{Ld(-)} \\ v_{Lq(-)} \\ v_{L0(-)} \end{bmatrix} = \frac{2}{3} \begin{bmatrix} \cos(-\omega t) & \cos(-\omega t - \frac{2\pi}{3}) & \cos(-\omega t + \frac{2\pi}{3}) \\ \sin(-\omega t) & -\sin(-\omega t - \frac{2\pi}{3}) & -\sin(-\omega t + \frac{2\pi}{3}) \\ \frac{1}{2} & \frac{1}{2} & \frac{1}{2} \end{bmatrix} \begin{bmatrix} v_{La} \\ v_{Lb} \\ v_{Lc} \end{bmatrix} \quad (7)$$

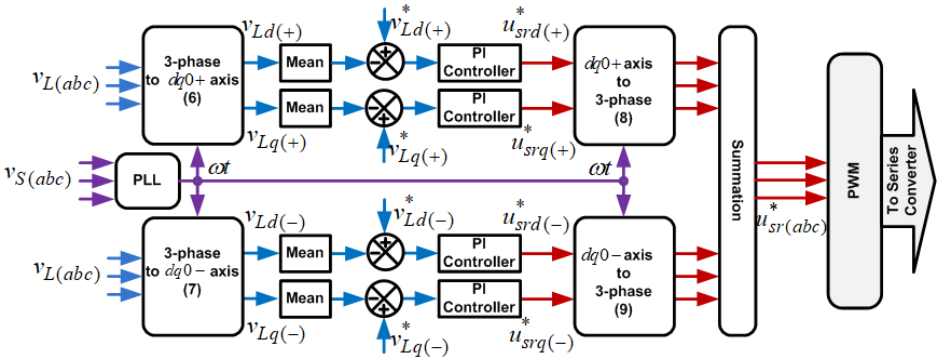

Figure 5. Control block diagram of series converter of UPQC

Certainly, converting a three-phase *abc* signal into a *dq0* rotating reference frame in an unbalanced system will result in a *dq0* signal that is an imperfect DC signal. In other words, this signal will oscillate at

twice the frequency of the fundamental frequency. To achieve a perfectly DC signal, it is necessary to apply a process that averages out the given signal. To achieve balance in the two-phase load voltage (v_{Lab} and v_{Lcb}), it is essential to regulate the *dq*-NSC components to zero ($v^*_{Ld(-)} = 0$ and $v^*_{Lq(-)} = 0$). In the meantime, the *dq*-PSC is utilized to adjust the load voltage to the preset level, where the desired voltage magnitude depends on $|v_L| = \sqrt{(v^*_{Ld(+)})^2 + (v^*_{Lq(+)})^2}$ and the voltage angle is related to $ang(v_L) = \tan^{-1}\left(v^*_{Lq(+)}/v^*_{Ld(+)}\right)$.

$$\begin{bmatrix} u^*_{sra(+)} \\ u^*_{srb(+)} \\ u^*_{src(+)} \end{bmatrix} = \begin{bmatrix} \cos(\omega t) & -\sin(\omega t) & 1 \\ \cos(\omega t - \frac{2\pi}{3}) & -\sin(\omega t - \frac{2\pi}{3}) & 1 \\ \cos(\omega t + \frac{2\pi}{3}) & -\sin(\omega t + \frac{2\pi}{3}) & 1 \end{bmatrix} \begin{bmatrix} u^*_{srd(+)} \\ u^*_{srq(+)} \\ u^*_{sr0(+)} \end{bmatrix} \tag{8}$$

$$\begin{bmatrix} u^*_{sra(-)} \\ u^*_{srb(-)} \\ u^*_{src(-)} \end{bmatrix} = \begin{bmatrix} \cos(-\omega t) & -\sin(-\omega t) & 1 \\ \cos(-\omega t - \frac{2\pi}{3}) & -\sin(-\omega t - \frac{2\pi}{3}) & 1 \\ \cos(-\omega t + \frac{2\pi}{3}) & -\sin(-\omega t + \frac{2\pi}{3}) & 1 \end{bmatrix} \begin{bmatrix} u^*_{srd(-)} \\ u^*_{srq(-)} \\ u^*_{sr0(-)} \end{bmatrix} \tag{9}$$

The series converter control employs four proportional-integral (PI) controllers for its operation. The outputs of the PI controllers serve as the reference signals for the *dq*-PSC and *dq*-NSC components of the series converter ($u^*_{srd(+)}$, $u^*_{srq(+)}$, $u^*_{srd(-)}$ and $u^*_{srq(-)}$). The referenced signals of the *dq*-PSC and *dq*-NSC are converted back to positive and negative components three-phase AC signals through (8) and (9), respectively. Note that for a three-phase three-wire system, the zero-sequence component can be neglected ($u^*_{sr0(+)} = u^*_{sr0(-)} = 0$). Subsequently, the three-phase AC referenced signals of the series converter ($u^*_{sr(abc)}$) can be acquired by summing these transformed reference signals. The series converter requires gate pulses which are generated using pulse width modulation (PWM).

3.3. System parameter and PI controller design

Based on the single-line diagram illustrated in Figure 3, the system's equivalent circuit, including the right-shunt UPQC, is presented in Figure 6. In this equivalent circuit, the railway load is modeled as a series combination of resistance and inductance. The parameters for both the system and the UPQC are provided in Table 1.

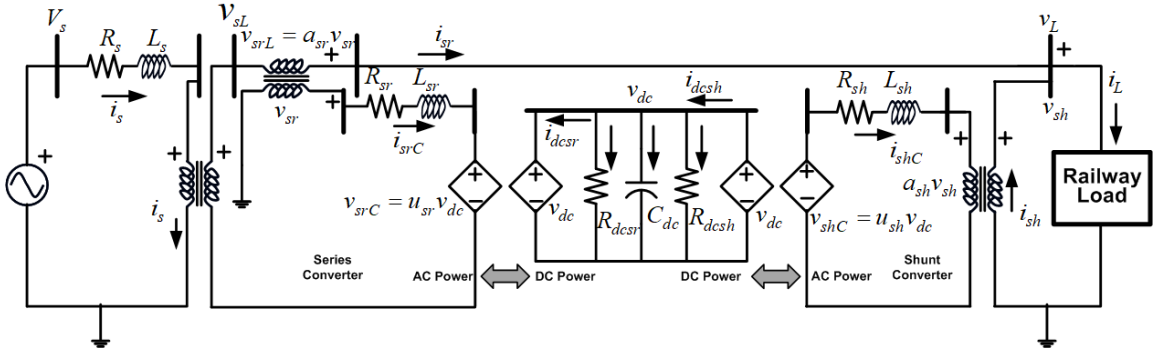

Figure 6. Equivalent circuit of the system

Table 1. System and UPQC parameters

Parameter name	Symbol	Value	Unit	Parameter name	Symbol	Value	Unit
Source voltage	V_s	115	kV	Series transformer ratio	a_{sr}	6/1	-
V/V transformer ratio	a_v	25/115	-	Series resistance	R_{sr}	0.001	Ω
Source resistance	R_s	0.02	Ω	Series inductance	L_{sr}	0.1	mH
Source inductance	L_s	0.5	mH	DC losses resistance	R_{dcsr}, R_{dcsh}	100, 100	Ω
Norminal load voltage	v_L	25	kV	Norminal DC voltage	v_{dc}	3.00	kV
Load train 1	P_{L1}+jQ_{L1}	4.0+j0.65	MVA	DC capacitance	C_{dc}	80,000	μF
Load train 2	P_{L2}+jQ_{L2}	2.5+j0.30	MVA	Shunt resistance	R_{sh}	0.001	Ω
Shunt transformer ratio	a_{sh}	1/25	-	Shunt inductance	L_{sh}	0.1	mH
Fundamental frequency	f_n	50	Hz	Switching frequency	f_s	10	kHz

When examining the equivalent circuit of a series converter shown in Figure 6, the formula for the output voltage, v_{srL}, at the series transformer in dq-PSC and dq-NSC can be expressed in the following manner:

$$v_{srLd(\pm)} = a_{sr} v_{srd(\pm)} = a_{sr}(v_{srCd(\pm)} - R_{sr} i_{srCd(\pm)} + \omega L_{sr} i_{srCq(\pm)}) \quad (10)$$

$$v_{srLq(\pm)} = a_{sr} v_{srq(\pm)} = a_{sr}(v_{srCq(\pm)} - R_{sr} i_{srCq(\pm)} - \omega L_{sr} i_{srCd(\pm)}) \quad (11)$$

The subscribe $(\pm)$ means the positive and negative components. The both dq-PSC and dq-NSC axes of the voltage v_{srC} at the series converter can be modified by controlling the signal u_{sr} in dq-PSC and dq-NSC axes as well. However, the voltage v_{srL} is used to enhance the load voltage by combining it with the supply voltage v_{sL}. Consequently, the load voltage, v_L, in dq-PSC and dq-NSC axes can be represented by the following equations.

$$v_{Ld(\pm)} = v_{sLd(\pm)} = a_{sr}(u_{srd(\pm)} v_{dc} - R_{sr} i_{srCd(\pm)} + \omega L_{sr} i_{srCq(\pm)}) \quad (12)$$

$$v_{Lq(\pm)} = v_{sLq(\pm)} = a_{sr}(u_{srq(\pm)} v_{dc} - R_{sr} i_{srCq(\pm)} + \omega L_{sr} i_{srCd(\pm)}) \quad (13)$$

As shown in (12) through (13), the signal u_{sr} functions as the input, while the voltage v_L is regarded as the output of control systems. The diagram illustrating the control mechanism for adjusting the load voltage of the series converter as shown in Figure 7. As mentioned earlier, the unbalanced transformation of three-phase voltage on the dq-PSC and dq-NSC axes results in the creation of oscillating signals twice the fundamental frequency. Hence, utilizing averaging methods becomes essential to regulate this load voltage. This averaging is expressed through a constant-time transfer function, characterized by a time constant of $T_{mean} = 0.005$.

Based on the control diagram depicted in Figure 7 and the system parameters outlined in Table 1, the transfer function of the load voltage control system, neglecting any disturbances ($i_{srC}R_{sr}$, $i_{srC}\omega L_{sr}$, and v_{sL}) can be expressed by the (14).

$$\frac{V_L(s)}{U_{sr}(s)} = \frac{12{,}000}{0.005s+1} \quad (14)$$

Through the design of a PI controller aimed at ensuring robust response time with a phase margin (P.M.) exceeding 60 degrees and a gain margin (G.M.) surpassing 6 dB, the controller's P and I component parameters are established at $K_P = 0.00008$ and $K_I = 0.052$. To design the PI controller for DC voltage regulation, we employ the mathematical model of the DC voltage of the UPQC, detailed in [45], which can be expressed by (15).

$$\frac{dv_{dc}}{dt} = -\frac{1}{C_{dc}R_{dcsh}} v_{dc} - \frac{1}{C_{dc}R_{dcsr}} v_{dc} + \frac{3}{2}\frac{1}{C_{dc}v_{dc}} v_{shC} i_{shC} \quad (15)$$

In this context, C_{dc} represents the DC link capacitor, while R_{dcsh} and R_{dcsr} denote losses in the shunt and series converters, with $R_{dcsh} = R_{dcsr}$ simplifying the design. The control system is based on a fixed current $i_{shC} = I_{shC}$ with the shunt converter voltage $v_{shC} = u_{sh} v_{dc}$. Using these parameters, the DC voltage control system schematic as shown in Figure 8 is developed. Based on this diagram and Table 1, the transfer function for the system, under nominal conditions with I_{shC}=50 A, is given in (16).

$$\frac{V_{dc}(s)}{U_{sh}(s)} = \frac{3}{2}\frac{50\times100}{(80{,}000\times10^{-6}\times100s+2)(0.005s+1)} \quad (16)$$

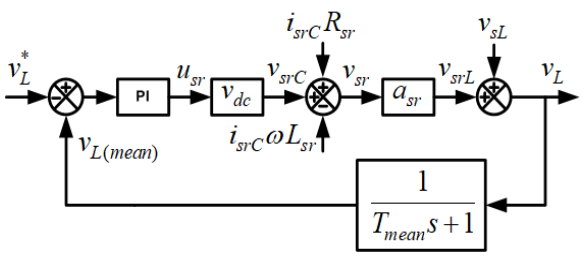

Figure 7. Block diagram of load voltage control

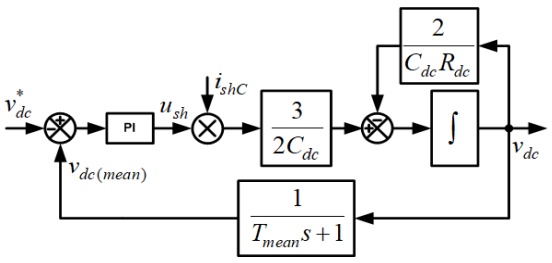

Figure 8. Block diagram of DC voltage control

To achieve a robust and stable response in the DC voltage control system, a proportional-integral (PI) controller is meticulously designed. The primary objective of this design is to ensure a phase margin (P.M.) greater than 60 degrees and a gain margin (G.M.) exceeding 6 dB, which collectively contribute to improved system stability and dynamic performance. Through an iterative tuning process that considers the system's dynamics and control objectives, the proportional and integral gains of the PI controller are determined as $K_P = 0.1232$ and $K_I = 0.16645$, respectively. These parameters are selected to optimize both transient response and steady-state error correction, ensuring the controller meets the desired performance criteria.

4. SIMULATION RESULTS

This section presents the results of testing a UPQC for improving unbalanced currents and voltage stability in railway electrification system using MATLAB simulations. Figure 9 illustrates the test system simulated using MATLAB, with the parameters detailed in Table 1. Four case studies were evaluated: i) integration of UPQC, ii) increased train load, iii) single phase-to-ground fault, and iv) unbalance three phase-to-ground fault. Results highlight UPQC's superior performance, with detailed analysis supported by graphs and numerical data demonstrating its effectiveness in enhancing power quality and ensuring stability across all scenarios.

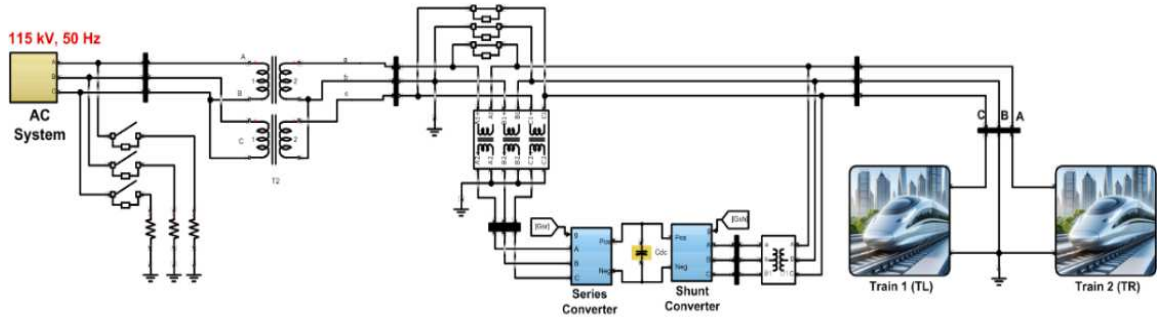

Figure 9. Test system simulated using MATLAB

4.1. Integration of UPQC

This test focuses on evaluating the capability of UPQC in managing unbalanced currents during the initial startup phase of compensation. During the time interval from t=0.1 – 0.2 seconds, the system operates with only the train 1 (TL) active. As depicted in Figure 10, the train 1 draws current from phase-a of the system and returns it through phase-b, while phase-c remains unloaded. During this period, the three-phase supply currents exhibit a significant imbalance, reaching 100%. Furthermore, the system experiences substantial harmonic distortion, with the total harmonic distortion (THD) measured at 10.26%.

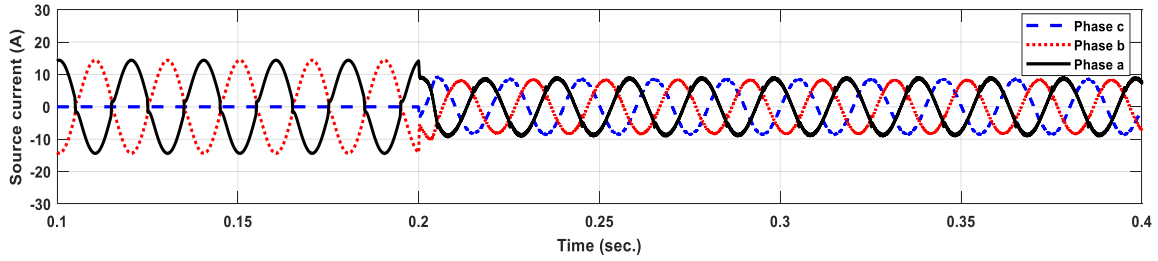

Figure 10. Managing unbalanced currents during the initial startup phase of compensation

At t=0.2 seconds, the UPQC is activated in the system. Simulation results reveal that the UPQC effectively addresses the current imbalance by injecting three-phase compensating currents through its shunt converter, as illustrated in Figure 11. Consequently, the three-phase supply currents are restored to a balanced state, reducing the imbalance percentage to 3.025%, as depicted in Figure 10 at t=0.2 – 0.4 seconds.

Moreover, the UPQC significantly reduces harmonic distortion, lowering the THD to 4.89%. These findings highlight the UPQC's capability to enhance power quality by mitigating current imbalances and harmonic distortions, even under challenging system conditions.

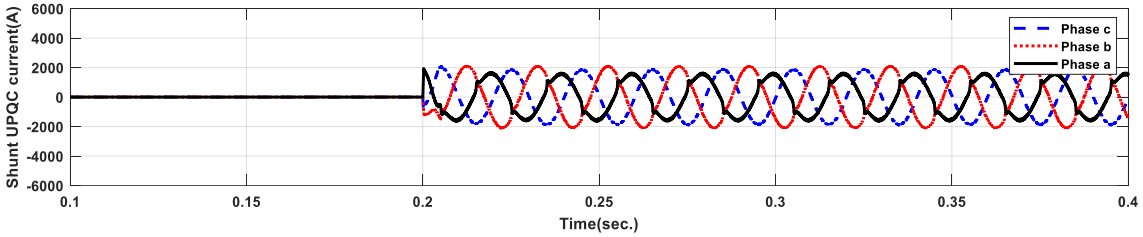

Figure 11. Shunt converter currents during the initial startup phase of compensation

4.2. Increased train load

This study examines the effects of increased load on the system, specifically at t=1.0 seconds, when the second train (TR) is introduced into the network. The simulation results shown in Figure 12 indicate that the system current increases from about 9A to 14A at t=1.0 seconds. During this interval, the UPQC demonstrates its effectiveness in compensating for both current imbalance and harmonic distortion.

The compensating current generated by the UPQC under these conditions is illustrated in Figure 13. While the magnitude of the compensating current remains comparable to the previous case, its waveform exhibits slight variations due to changes in the current consumption behavior of the train. The UPQC's compensation leads to a substantial decrease in the current imbalance, achieving an imbalance percentage of 1.6%, and a substantial decrease in the THD to 2.42%. A detailed analysis of harmonic currents is highlighting the UPQC's capability to enhance power quality in the presence of dynamic load variations.

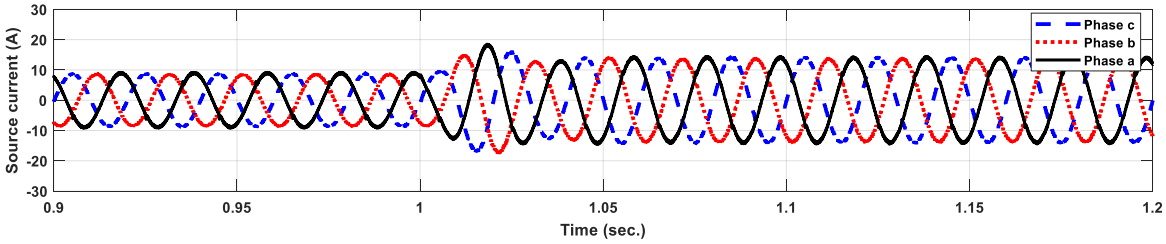

Figure 12. Managing unbalanced currents for increasing train load

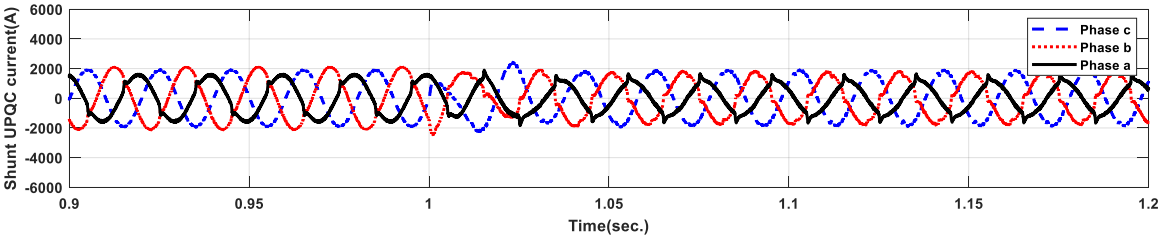

Figure 13. Shunt converter currents for increasing train load

4.3. Single phase-to-ground fault

This section describes the simulation of a single-phase-to-ground fault occurring on the source side at phase-a at 1.5 seconds. During this period, the rms voltage of phase-a on the source side decreases from 115 kV to 45.30 kV, as illustrated in Figure 14. Meanwhile, the rms voltages of the remaining phases remain at the normal value of 115 kV. This voltage sag causes the rms voltage supplied to the left train load (RL) to drop from 25.00 kV to 18.80 kV.

When the electric railway system is compensated using the series converter of a UPQC, the train 1 (TL) load voltage can be maintained at the desired 25kV. The voltage waveforms demonstrating this compensation are shown in Figure 15. Figure 16 presents the output voltage waveforms of the UPQC injected into the system to stabilize the load voltage. It is evident that the injected voltage is applied only to phase-a.

Regarding source current quality improvement during this fault, the results are depicted in Figure 17. The UPQC not only compensates the load voltage but also mitigates supply current issues, addressing both unbalance and harmonic distortions simultaneously. During this period, the supply current's unbalance percentage is reduced to 1.30%, and the THD is minimized to 2.49%. Nevertheless, a slight rise in source current is observed due to the increased power losses in the UPQC while compensating during fault conditions in the system. The waveforms of the compensated currents provided by the UPQC are shown in Figure 18.

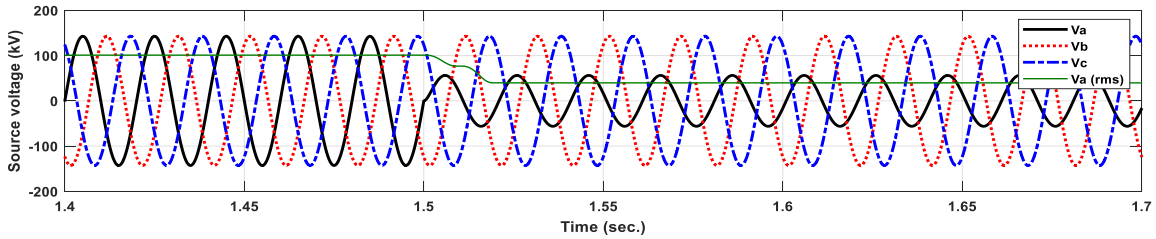

Figure 14. Source voltage for single phase-to-ground fault

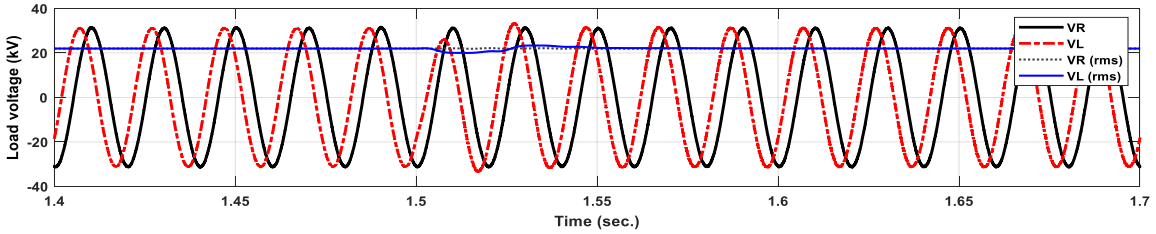

Figure 15. Load voltage for single phase-to-ground fault

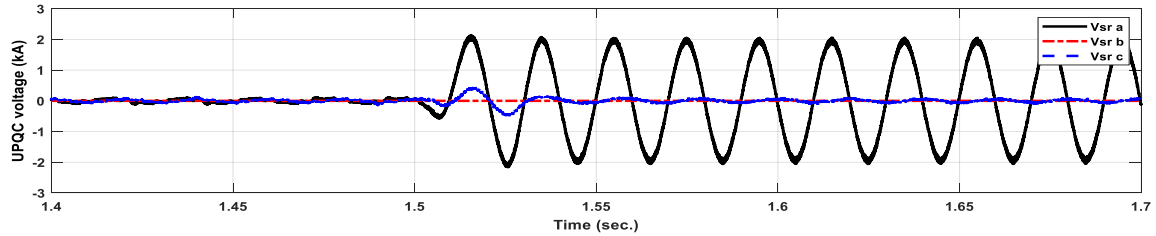

Figure 16. UPQC voltage for single phase-to-ground fault

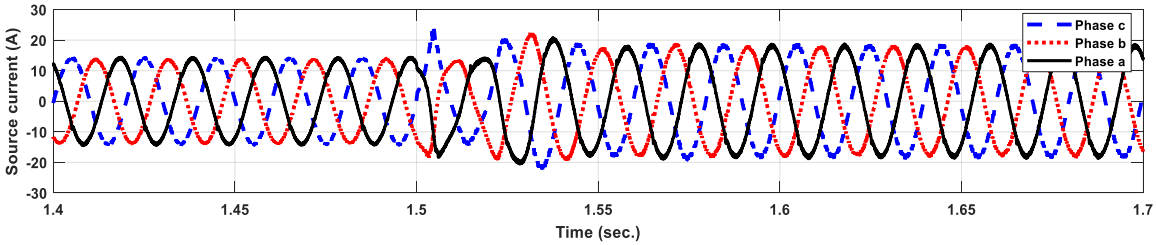

Figure 17. Source currents for single phase-to-ground fault

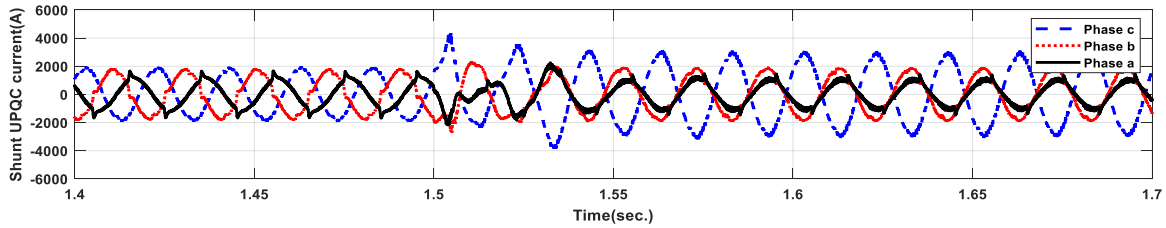

Figure 18. UPQC current for single phase-to-ground fault

4.4. Unbalance three phase-to-ground fault

This section details the simulation of an unbalanced three-phase-to-ground fault occurring on the source side at 1.5 seconds. During this fault, the rms voltage of phases-a, phases-b, and phases-c on the source side decreases from 115 kV to 76.00 kV, 71.13 kV, and 64.88 kV, respectively, as shown in Figure 19. This voltage sag results in a reduction of the rms voltage supplied to the left train load (RL) and the right train load (TR) from 25 kV to 15.70 kV and 15.36 kV, respectively.

When the electric railway system is compensated using the series converter of a UPQC, the voltage levels for both the left train load (TL) and the right train load (TR) are maintained at the set value of 25 kV. The voltage waveforms illustrating this compensation can be seen in Figure 20. Figure 21 displays the output voltage waveforms from the UPQC that are injected into the system to stabilize the load voltage, with compensation applied to phases a and c.

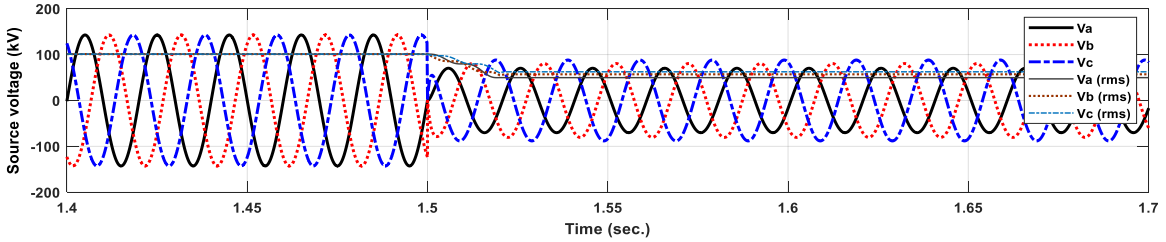

Figure 19. Source voltage for unbalance three phase-to-ground fault

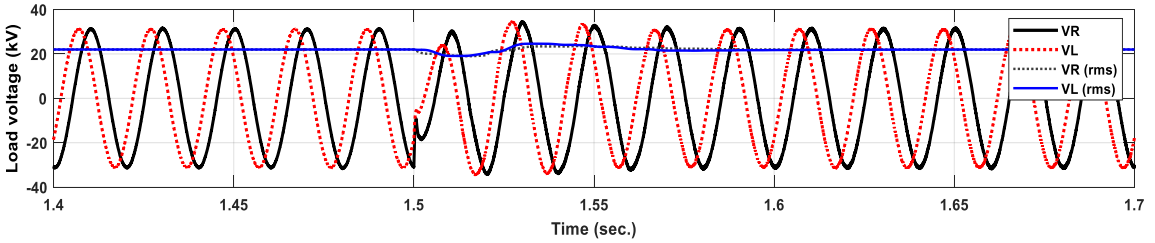

Figure 20. Load voltage for unbalance three phase-to-ground fault

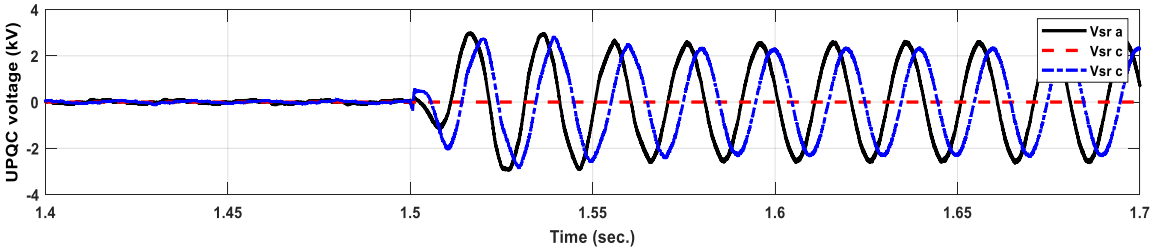

Figure 21. UPQC voltage for unbalance three phase-to-ground fault

For improving the source current quality during this fault condition, Figure 22 presents the outcomes. The UPQC not only maintains the load voltage stability but also corrects supply current imbalances and reduces harmonic distortions. The unbalance percentage of the supply current is brought down to 0.85%, and the THD is minimized to 2.43%. A slight increase in the source current is observed due to the additional power losses incurred by the UPQC while compensating for under three-phase fault conditions. These losses are more significant compared to those associated with single phase-to-ground faults. The current waveforms compensated by the UPQC are shown in Figure 23.

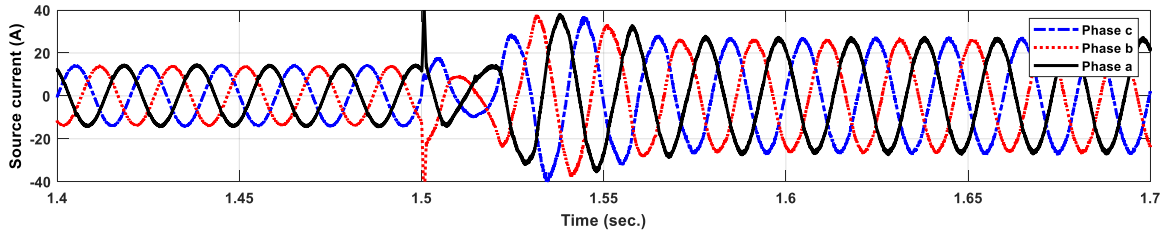

Figure 22. Source currents for unbalance three phase-to-ground fault

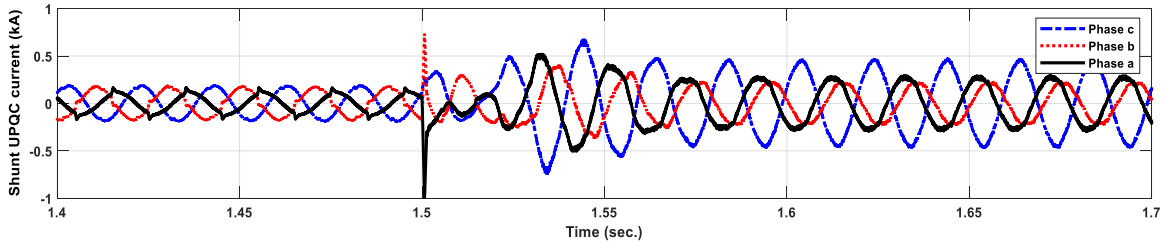

Figure 23. UPQC currents for unbalance three phase-to-ground fault

5. CONCLUSION

This research addresses critical power quality issues in railway electrification system, particularly those connected to low-voltage systems, by implementing a UPQC. The study highlights the UPQC's significant advancements in managing unbalanced currents, reducing current harmonics, and ensuring voltage stability, thereby enhancing the reliability and efficiency of electric railway operations. Railway electrification system, favored for their environmental benefits and cost efficiency, face challenges such as unbalanced currents and voltage fluctuations due to the use of single-phase transformers in a three-phase power supply system. The proposed UPQC, consisting of two three-phase power converters (shunt and series) connected in a back-to-back configuration with a shared DC capacitor, effectively mitigates these issues. The shunt converter addresses current imbalances and improves current harmonics by injecting compensating currents, while the series converter manages voltage fluctuations by injecting compensating voltages. The control strategies for the UPQC are based on instantaneous power theory for the shunt converter and synchronous rotating reference frame theory for the series converter, enabling real-time compensation and dynamic response to load changes and fault conditions. Comprehensive simulation results validate the UPQC's effectiveness in various scenarios, including increased train load and fault conditions, demonstrating significant reductions in THD and current imbalance percentages. The study also emphasizes the cost-effectiveness of the UPQC, which can be installed on the low-voltage side of the V/V transformer without extensive infrastructure modifications. The findings underscore the UPQC's potential for widespread adoption in railway electrification system, offering a robust solution for managing power quality challenges and improving system stability and efficiency. This research contributes valuable insights into the application of advanced power quality conditioners in transportation systems, paving the way for future developments in this field.

REFERENCES

[1] T. Trongjai, T. Narongrit, K. Areerak, and S. Janpong, "The comparison of three-phase and co-phase shunt active power filters for harmonic elimination in AC electric railway systems," in *2021 9th International Electrical Engineering Congress (iEECON)*, Mar. 2021, pp. 113–116, doi: 10.1109/iEECON51072.2021.9440353.

[2] Y. Wang, Y. He, X. Chen, M. Zhao, and J. Xie, "A layered compensation optimization strategy of energy storage type railway power conditioner," *Archives of Electrical Engineering*, vol. 71, no. 1, pp. 5–20, 2022, doi: 10.24425/aee.2022.140194.
[3] N. Gunavardhini and M. Chandrasekaran, "Power quality conditioners for railway traction—a review," *Automatika*, vol. 57, no. 1, pp. 150–162, 2016, doi: 10.7305/automatika.2016.07.966.
[4] H. J. Kaleybar, M. Brenna, F. Foiadelli, S. S. Fazel, and D. Zaninelli, "Power quality phenomena in electric railway power supply systems: An exhaustive framework and classification," *Energies*, vol. 13, no. 24, 2020, doi: 10.3390/en13246662.
[5] M. Brenna, F. Foiadelli, and D. Zaninelli, "Electrical railway transportation systems," *Electrical Railway Transportation Systems*, 2018, doi: 10.1002/9781119386827.
[6] P. E. Sutherland, M. Waclawiak, and M. F. McGranaghan, "System impacts evaluation of a single-phase traction load on a 115-kV transmission system," *IEEE Transactions on Power Delivery*, vol. 21, no. 2, pp. 837–844, 2006, doi: 10.1109/TPWRD.2006.873126.
[7] J. Wang *et al.*, "Power quality distribution characteristics analysis for multi-electrified railway traction load based on improved Gaussian mixture models with merging operator," in *2016 5th International Conference on Sustainable Energy and Environment Engineering (ICSEEE 2016)*, 2016, doi: 10.2991/icseee-16.2016.102.
[8] H. E. Mazin and W. Xu, "Harmonic cancellation characteristics of specially connected transformers," *Electric Power Systems Research*, vol. 79, no. 12, pp. 1689–1697, 2009, doi: 10.1016/j.epsr.2009.07.006.
[9] S. M. M. Gazafrudi, A. T. Langerudy, E. F. Fuchs, and K. Al-Haddad, "Power quality issues in railway electrification: A comprehensive perspective," *IEEE Transactions on Industrial Electronics*, vol. 62, no. 5, pp. 3081–3090, 2015, doi: 10.1109/TIE.2014.2386794.
[10] R. Targosz and D. Chapman, "Application note The cost of poor power quality," *Leonardo Energy*, no. October, pp. 1–24, 2012.
[11] L. A. M. Barros, M. Tanta, A. P. Martins, J. L. Afonso, and J. G. Pinto, "Evaluation of static synchronous compensator and rail power conditioner in electrified railway systems using V/V and Scott power transformers," *EAI Endorsed Transactions on Energy Web*, vol. 8, no. 34, pp. 1–17, 2021, doi: 10.4108/eai.29-3-2021.169164.
[12] S.-L. Chen, R.-J. Li, and P.-H. Hsi, "Traction system unbalance problem—analysis methodologies," *IEEE Transactions on Power Delivery*, vol. 19, no. 4, pp. 1877–1883, Oct. 2004, doi: 10.1109/TPWRD.2004.829920.
[13] Y. Danwen, L. Guanglei, W. Weixu, and W. Qingyu, "Power quality pre-evaluation method considering the impact of electrified railway," in *Proceedings - 2021 6th Asia Conference on Power and Electrical Engineering, ACPEE 2021*, 2021, pp. 1556–1559, doi: 10.1109/ACPEE51499.2021.9436913.
[14] L. Hu, R. E. Morrison, and D. J. Young, "Reduction of harmonic distortion and improvement of voltage form factor in compensated railway systems by means of a single arm filter," in *ICHPS 1992 - International Conference on Harmonics in Power Systems*, 1992, pp. 83–88, doi: 10.1109/ICHPS.1992.559001.
[15] A. Bueno, J. M. Aller, J. Restrepo, and T. Habetler, "Harmonic and balance compensation using instantaneous active and reactive power control on electric railway systems," in *Conference Proceedings - IEEE Applied Power Electronics Conference and Exposition - APEC*, 2010, pp. 1139–1144, doi: 10.1109/APEC.2010.5433358.
[16] Y. Sun, C. Dai, and J. Li, "A hybrid compensation method for electric railway's power quality improvement," in *Proceedings of the 5th IEEE International Conference on Electric Utility Deregulation, Restructuring and Power Technologies, DRPT 2015*, 2016, pp. 2287–2292, doi: 10.1109/DRPT.2015.7432627.
[17] H. J. Kaleybar, H. M. Kojabadi, M. Brenna, F. Foiadelli, and S. S. Fazel, "An active railway power quality compensator for 2×25kV high-speed railway lines," in *2017 IEEE Industrial and Commercial Power Systems Europe*, 2017, doi: 10.1109/EEEIC.2017.7977679.
[18] C. P. Huang, C. J. Wu, Y. S. Chuang, S. K. Peng, J. L. Yen, and M. H. Han, "Loading characteristics analysis of specially connected transformers using various power factor definitions," *IEEE Transactions on Power Delivery*, vol. 21, no. 3, pp. 1406–1413, 2006, doi: 10.1109/TPWRD.2005.864076.
[19] Z. Zhang, B. Wu, J. Kang, and L. Luo, "A multi-purpose balanced transformer for railway traction applications," *IEEE Transactions on Power Delivery*, vol. 24, no. 2, pp. 711–718, 2009, doi: 10.1109/TPWRD.2008.2008491.
[20] H. Jafarikaleybar, R. Kazemzadeh, and S. Farshad, "Power rating reduction of railway power quality compensator using steinmetz theory," in *6th Annual International Power Electronics, Drive Systems, and Technologies Conference, PEDSTC 2015*, 2015, pp. 442–447, doi: 10.1109/PEDSTC.2015.7093315.
[21] S. R. Huang and B. N. Chen, "Harmonic study of the Le Blanc transformer for Taiwan railway's electrification system," *IEEE Transactions on Power Delivery*, vol. 17, no. 2, pp. 495–499, 2002, doi: 10.1109/61.997925.
[22] M. Tanta, V. Monteiro, T. J. C. Sousa, A. P. Martins, A. S. Carvalho, and J. L. Afonso, "Power quality phenomena in electrified railways: Conventional and new trends in power quality improvement toward public power systems," in *Proceedings - 2018 International Young Engineers Forum, YEF-ECE 2018*, 2018, pp. 25–30, doi: 10.1109/YEF-ECE.2018.8368934.
[23] D. Serrano-Jiménez, L. Abrahamsson, S. Castaño-Solís, and J. Sanz-Feito, "Electrical railway power supply systems: Current situation and future trends," *International Journal of Electrical Power and Energy Systems*, vol. 92, pp. 181–192, 2017, doi: 10.1016/j.ijepes.2017.05.008.
[24] H. Wang, Y. Liu, K. Yan, Y. Fu, and C. Zhang, "Analysis of static VAr compensators installed in different positions in electric railways," *IET Electrical Systems in Transportation*, vol. 5, no. 3, pp. 129–134, 2015, doi: 10.1049/iet-est.2014.0046.
[25] G. Zhu, J. Chen, and X. Liu, "Compensation for the negative-sequence currents of electric railway based on SVC," in *2008 3rd IEEE Conference on Industrial Electronics and Applications, ICIEA 2008*, 2008, pp. 1958–1963, doi: 10.1109/ICIEA.2008.4582862.
[26] M. Jianzong, W. Mingli, and Y. Shaobing, "The application of SVC for the power quality control of electric railways," in *1st International Conference on Sustainable Power Generation and Supply, SUPERGEN '09*, 2009, doi: 10.1109/SUPERGEN.2009.5347939.
[27] Q. Zhang, G. Liu, and Y. Pang, "Control method of STATCOM for electric railway," *World Automation Congress Proceedings*, 2012.
[28] P. Rodrigues, V. A. Morais, A. Martins, and A. Carvalho, "STATCOM simulation models for analysis of electrified railways," in *IECON Proceedings (Industrial Electronics Conference)*, vol. 2019-Octo, pp. 2257–2262, 2019, doi: 10.1109/IECON.2019.8927256.
[29] A. Luo, F. Ma, C. Wu, S. Q. Ding, Q. C. Zhong, and Z. K. Shuai, "A dual-loop control strategy of railway static power regulator under V/V electric traction system," *IEEE Transactions on Power Electronics*, vol. 26, no. 7, pp. 2079–2091, 2011, doi: 10.1109/TPEL.2010.2103383.
[30] Y. Li, J. Hu, Z. Tang, Y. Xie, and F. Zhou, "Feedforward compensation of railway static power conditioners in a V/V traction power supply system," *Electronics (Switzerland)*, vol. 10, no. 6, pp. 1–18, 2021, doi: 10.3390/electronics10060656.
[31] S. Hu, Z. Zhang, Y. Li, L. Luo, and P. Luo, "An LC-coupled electric railway static power conditioning system," *Diangong Jishu Xuebao/Transactions of China Electrotechnical Society*, vol. 31, no. 8, pp. 199–211, 2016.
[32] H. Morimoto *et al.*, "Development of railway static power conditioner used at substation for Shinkansen," in *Proceedings of the Power Conversion Conference-Osaka 2002, PCC-Osaka 2002*, 2002, vol. 3, pp. 1108–1111, doi: 10.1109/PCC.2002.998127.

[33] Z. Sun, X. Jiang, D. Zhu, and G. Zhang, "A novel active power quality compensator topology for electrified railway," *IEEE Transactions on Power Electronics*, vol. 19, no. 4, pp. 1036–1042, 2004, doi: 10.1109/TPEL.2004.830032.
[34] N. Dai, K. Lao, and M. Wong, "A hybrid railway power conditioner for traction power supply system," in *Conference Proceedings - IEEE Applied Power Electronics Conference and Exposition - APEC*, pp. 1326–1331, 2013, doi: 10.1109/APEC.2013.6520471.
[35] L. Liu, N. Y. Dai, and X. Zeng, "Hybrid railway power conditioner based on chopper cell modular multilevel converter with four legs," *2017 20th International Conference on Electrical Machines and Systems, ICEMS 2017*, 2017, doi: 10.1109/ICEMS.2017.8055962.
[36] C. Che *et al.*, "Analysis, design and control of a hybrid railway power conditioner considering power rating reduction," *Electric Power Systems Research*, vol. 227, 2024, doi: 10.1016/j.epsr.2023.109895.
[37] F. Ma, A. Luo, X. Xu, C. Wu, Z. Shuai, and X. Yang, "High-power hybrid power quality compensation system in electrified railway," *Diangong Jishu Xuebao/Transactions of China Electrotechnical Society*, vol. 26, no. 10, pp. 93–102, 2011.
[38] R. Sinha, H. A. Vidya, and H. R. Sudarshan Reddy, "Unified power quality conditioner for V/V connected electrified railway traction power supply system," *Cognitive Science and Technology*, pp. 263–277, 2023, doi: 10.1007/978-981-19-8086-2_26.
[39] K. Srilakshmi, K. Kondreddi, A. Ramadevi, R. Muniraj, and R. Vangalapudi, "Grid connected and standalone renewable source fed UPQC: a hybrid control technique for power quality enhancement," *Discover Applied Sciences*, vol. 7, no. 3, 2025, doi: 10.1007/s42452-025-06562-9.
[40] D. K. Nishad, A. N. Tiwari, S. Khalid, and S. Gupta, "Power quality solutions for rail transport using AI-based unified power quality conditioners," *Discover Applied Sciences*, vol. 6, no. 12, 2024, doi: 10.1007/s42452-024-06372-5.
[41] D. K. Nishad, A. N. Tiwari, S. Khalid, S. Gupta, and A. Shukla, "AI based UPQC control technique for power quality optimization of railway transportation systems," *Scientific Reports*, vol. 14, no. 1, 2024, doi: 10.1038/s41598-024-68575-5.
[42] H. Akagi, E. H. Watanabe, and M. Aredes, "Instantaneous power theory and applications to power conditioning," *Instantaneous Power Theory and Applications to Power Conditioning*, pp. 1–379, 2006, doi: 10.1002/0470118938.
[43] A. Ghosh and G. Ledwich, "Power quality enhancement using custom power devices," *Power Quality Enhancement Using Custom Power Devices*, 2002, doi: 10.1007/978-1-4615-1153-3.
[44] B. Blazic and I. Papic, "Improved D-StatCom control for operation with unbalanced currents and voltages," *IEEE Transactions on Power Delivery*, vol. 21, no. 1, pp. 225–233, 2006.
[45] X. Xu, L. Li, Y. Wang, Y. Xie, X. Zhang, and Z. Zeng, "Novel unified power quality conditioner (UPQC) of two DC links connected with resistor," in *2016 IEEE International Conference on Renewable Energy Research and Applications, ICRERA 2016*, pp. 590–594, 2016, doi: 10.1109/ICRERA.2016.7884403.

BIOGRAPHIES OF AUTHORS

Kittaya Somsai is currently an assistant professor in the Department of Electrical Engineering, Rajamangala University of Technology Isan (RMUTI) Sakon Nakhon Campus, Thailand. He received the B.Eng. in electrical engineering from Rajamangala's Institute of Technology, Thailand (2003), M.Eng in Electrical Engineering from King Mongkut's Institute of Technology North Bangkok (KMITNB), Thailand (2005), and Ph.D. in electrical engineering from Suranaree University of Technology, Thailand (2012). His research fields are interested in power systems, custom power devices, power electronics and control, and artificial intelligence techniques. He can be contacted at email: kittaya.so@rmuti.ac.th.

Jeerapong Srivichai is a lecturer of the Department of Electrical Engineering, Rajamangala University of Technology Isan (RMUTI) Sakon Nakhon Campus, Thailand. He received the B.Eng in electrical engineering from Pathumwan Institute of Technology, Bangkok, Thailand. (2003), M.Eng. in electrical engineering from Kasetsart University, Bangkok, Thailand (2008), and Ph.D. in electrical engineering from Suranaree University of Technology, Thailand (2020). His research fields are interested in railway electrification, electric vehicle, power electronics, and induction heating. He can be contacted at email: geerapong.sr@rmuti.ac.th.

Veera Thanyaphirak received B.Eng. in electrical engineering from Rajamangala Institute of Technology, Pathumthani, Thailand, in 1996, and M.Eng. in electrical engineering from King Mongkut's Institute of Technology Ladkrabang, Bangkok, Thailand, in 2004. Since 2011, he has worked for his D.Eng. in electrical engineering at King Mongkut's Institute of Technology Ladkrabang, Bangkok, Thailand. His research interests include energy conversion, electrical machines and electric drives. He can be contacted at email: veera.th@rmuti.ac.th.